CHANSON, H., and TOOMBES, L. (1998). "Supercritical Flow at an Abrupt Drop : Flow Patterns and Aeration." *Can. Jl of Civil Eng.*, Vol. 25, No. 5, Oct., pp. 956-966 (ISSN 0315-1468).

# SUPERCRITICAL FLOW AT AN ABRUPT DROP : FLOW PATTERNS AND AERATION

by H. Chanson, Senior Lecturer, and L. Toombes, Ph.D. student

Dept. of Civil Engineering, The University of Queensland, Brisbane QLD 4072, Australia

**Abstract** : Stepped waterways and cascades are common features of storm waterways, at dam outlets and in water treatment plants. At an abrupt drop, open channel flows are characterised by the presence of shock waves and a substantial flow aeration. There is however little information on the basic flow characteristics. The study presents new experimental data obtained in a 0.5-m wide stepped flume with an un-ventilated nappe. The investigations describe the three-dimensional flow patterns (shock waves, standing waves, spray) downstream of the nappe impact. The characteristics of the flow patterns are similar to those observed with abrupt expansion supercritical flows. Downstream of the drop brink, substantial aeration takes place along the nappe interfaces and the flow downstream of the impact is de-aerated.

Keywords : Abrupt drop, supercritical flow, shockwaves, flow patterns, cascade.

## 1. Introduction

In storm waterways, at dam outlets and in water treatment plants, it is common to design drops, stepped waterways and cascades. At each drop, the supercritical flow takes off as a free-falling nappe before impacting onto the downstream invert. Substantial flow aeration (i.e. 'white water') is observed and there is little information on the air-water flow characteristics.

It is the purpose of this study to present new information on the supercritical flow at an abrupt drop and the free-surface aeration. The study is based on new experimental data obtained in a large channel at the University of Queensland. The results are compared with supercritical flows at an abrupt expansion and with prototype observations at the Gold Creek dam cascade (Australia).

## 2. Experimental apparatus and method

The authors conducted a series of new experiments in a 0.5-m wide channel (table 1). The flow is issued from an elliptical convergent and the drop, 0.131 m high, is located 2.4 m downstream of the nozzle. The flume is made of planed wooden boards (equivalent surface roughness height : 1 mm). The channel invert, upstream and downstream of the vertical drop, is flat and horizontal. An overfall is located 2.4-m downstream of the drop and prevents any form of backwater effect.

Water is supplied by a pump, with a variable-speed electronic controller (Taian™ T-verter K1-420-M3 adjustable frequency AC motor drive), enabling an accurate discharge adjustment in a closed-circuit system. Flow to the flume is fed through a smooth convergent nozzle (1.7-m long), and the nozzle exit is 30-mm high and 0.5-m wide. The measured contraction ratio is about unity (i.e. $d_o$ = 30 mm for all experiments). Earlier experiments (Chanson 1995) showed that the flow at the nozzle is two-dimensional.

CHANSON, H., and TOOMBES, L. (1998). "Supercritical Flow at an Abrupt Drop : Flow Patterns and Aeration." *Can. Jl of Civil Eng.*, Vol. 25, No. 5, Oct., pp. 956-966 (ISSN 0315-1468).

The water discharge is measured with a Dall™ tube flowmeter, calibrated on site. The accuracy on the discharge measurement is about 2%. Clear-water flow depths were measured with a point gauge. Air concentration measurements were performed using a single-tip conductivity probe developed at the University of Queensland (Chanson 1995). The probe consists of an internal concentric electrode of ∅ = 0.35 mm made of platinum and an external stainless steel electrode of 1.42 mm diameter. The probe is aligned in the flow direction and excited by an air bubble detector (AS25240). This electronic system was designed with a response time less than 10 μs and calibrated with a square wave generator.

The translation of the probe in the direction normal to the channel bottom was controlled by a fine adjustment travelling mechanism connected to a Mitutoyo™ digimatic scale unit (Ref. No. 572-503). The error on the vertical position of the probe was less than 0.025 mm. The system (probe and travelling mechanism) was mounted on a trolley system. The accuracy on the longitudinal position of the probe was estimated to $\Delta x < \pm 1$ cm. The accuracy on the transverse position of the probe was estimated as $\Delta z < \pm 1$ mm.

Nappe cavity subpressures were recorded with a projection manometer (TEM Engineering™ Ref.: M939). The accuracy of the manometer is about ±1 Pa. In addition high-speed photographs were taken to analyse the flow patterns. Further details of the instrumentation and the full set of experimental data were reported in Chanson and Toombes (1997).

## 3. Flow patterns

### 3.1 Presentation

With the abrupt drop geometry, experimental observations indicate that the water flows as a supercritical flow upstream and downstream of the abrupt drop for all the investigated flow conditions (table 1). At the end of the drop, the flow becomes a free-falling jet and the air cavity beneath the nappe was well established. Note that the air cavity was normally not ventilated. Nappe cavity subpressures are reported in table 1 (column 5). For one particular discharge (i.e. $q_W \approx 0.163$ m$^2$/s), loud noise occurred, generated by inadequate nappe ventilation lading to fluttering instabilities. The noise could be stopped by ventilating of the air cavity.

Observations showed that the approach flow and the free-falling nappe were basically two-dimensional. Downstream of the nappe impact, the flow became three-dimensional and white-water was observed (fig. 2).

### 3.2 Basic flow patterns

For all flow rates investigated, the jet impact induced significant water splashing and jet deflection, followed by the propagation of oblique shock waves or cross-waves intersecting further downstream on the channel centreline (fig. 1 and 2). The nappe impact on the horizontal step is characterised by a change of flow direction in the vertical streamwise plane and by some flow deceleration caused by energy dissipation at drop impact. The change of streamline direction in the supercritical flow induces the propagation of shock waves.

For $d_C/h < 0.84$, the shock waves are basically straight and intersect upstream of the downstream overfall (fig. 1(a) and 2(a)). For $d_C/h > 0.84$, the cross-waves are not straight. Each shock wave exhibits a broken line (fig. 1(c) and 2(d)). At the sidewall, the angle between the shockwave and the flow direction appears to be greater than the angle observed

further downstream. The decrease in shockwave angle seems to correspond to the location where the spray re-attaches to the mainstream (fig. 1(c)).

Standing waves are observed also at the impact of the nappe along the sidewalls (fig. 2(b)). Note that the location of maximum height of the wall standing waves does not coincide exactly with the start of the crosswaves.

For $d_C/h = 0.839$, the shock waves developing downstream of the nappe impact intersect at the brink of the downstream overfall (i.e. edge of second overfall). Immediately downstream of the shock wave intersection, a 'rooster tail' wave takes place on the centreline of the second free-falling nappe, 'riding' over the upper nappe (fig. 1(b) and 2(c)). For $d_C/h > 0.84$, the shock waves downstream of the drop intersect downstream of the brink of the overfall (fig. 1(c)).

3.3 Discussion

Overall significant jet deflection, shockwaves and standing waves are observed downstream of the drop. Interestingly two types of shock wave intersection are observed downstream of the drop. At low flow rates (i.e. $d_C/h < 0.66$), the crosswaves intersect without significant interference : this type is typical in non-aerated supercritical flows. For $d_C/h > 0.66$, the free-surface behind the shock waves is characterised by turbulent wavelets and the free-surface looks rougher downstream of the crosswaves.

## 4. Shock wave characteristics

The characteristics of the standing waves and of the cross-waves were recorded and the main results are presented in figures 3 to 6.

Figure 3 presents the dimensionless drop length $L_{drop}/W$, the location of the maximum standing wave free-surface elevation $(L_M)_{wall}/W$, position of the start of shock waves at the sidewall $(L_{sw})_{wall}/W$ and position of the intersection of shock waves $(L_{sw})_{int}/W$, where W is the downstream channel width. The data are plotted as functions of the downstream ideal flow Froude number Fr (see App. A), being the downstream Froude number in absence of energy dissipation.

Figure 3 indicates a consistent increase in dimensionless drop length and locations of the standing wave and cross-waves with increasing Froude number. The drop length data compare favourably with experimental data by Dominguez (1974, p. 390, fig. 196). They are best correlated by :

[1] $$\frac{L_{drop}}{W} = 0.21885 * (Fr - 3.1516)$$ (Data : Present study)

[2] $$\frac{(L_M)_{wall}}{W} = 2.983 * \frac{Fr + 3.933}{Fr^2 + 37.65} * (Fr - 3.933)$$ (Data : Present study)

[3] $$\frac{(L_{sw})_{wall}}{W} = 0.4426 * (Fr - 4.5096)$$ (Data : Present study)

[4] $$\frac{(L_{sw})_{int}}{W} = 0.705 * (Fr - 1.776)$$ (Data : Present study)

CHANSON, H., and TOOMBES, L. (1998). "Supercritical Flow at an Abrupt Drop : Flow Patterns and Aeration." *Can. Jl of Civil Eng.*, Vol. 25, No. 5, Oct., pp. 956-966 (ISSN 0315-1468).

For design of chutes and sewers, the wave heights are determining parameters. In figure 4 the dimensionless wave heights at the wall and at the shock wave intersection are plotted as functions of the downstream Froude number, where ($E = E_o + h$) is the upstream total head, taking the downstream channel bed as datum. The data are compared with re-analysed data of supercritical flows at channel expansions (table 2). Figure 4 shows a close agreement between the wave heights at an abrupt drop and at an abrupt expansion. At an abrupt drop, the impinging nappe experiences a change in momentum direction and some flow deceleration caused by energy dissipation. The flow pattern is somewhat similar to a supercritical flow at a sudden channel expansion. That is, the flow is subjected to a rapid change of streamline direction and a sudden deceleration with propagation of oblique shock waves and flow deflection along the sidewall. The data are best correlated by :

[5] $$\frac{(d_M)_{wall}}{E} = \frac{5.4305}{Fr^{2.003}}$$ (Data : Present study, Hager and Mazumder)

[6] $$\frac{(d_M)_{int}}{E} = 0.52613 * 0.77449^{Fr}$$

(Data : Present study, Hager and Mazumder, Mazumder and Hager)

The wave heights are a form of potential energy which account for 5 to 20% of the total energy of the flow. Note that the standing wave heights are consistently higher at the wall than on the centreline.

Figure 5 presents the dimensionless standing wave thickness (at maximum wave height) $t_{wall}/E$ versus the downstream Froude number Fr (eq. (9)). The data are compared with re-analysed data obtained at a 30-degree channel junction (table 2). Interestingly the standing wall thickness is of the same order of magnitude as the sidewall wave height (fig. 4 and 5). Note that the standing wave has a 'drop' shape (fig. 1) and its maximum thickness is located at its downstream end. Overall the data are best fitted by :

[7] $$\frac{t_{wall}}{E} = 0.00633 * (7.151\ E+5)^{1/(Fr-1)}$$ (Data : Present study)

The shock wave angle data are presented in figure 6 and compared with re-analysed data at channel expansions. In figure 6, the authors' data are presented in two series : the angle measured at the wall (∗) and the angle measured near the downstream overfall (×) after the re-attachment of spray for the largest discharges (fig. 1(c)).

For flows with a significant spray development, visual observations suggest that the rebounding waters re-attach to the main stream with impact velocities larger than the mean flow. If this hypothesis is verified, the flow immediately downstream of the impact would be slower than the spray, leading to a wider shock wave angle at the wall, as suggested by fig. 6. Overall the data downstream of the spray re-attachment show a decrease of shock wave angle with increasing Froude number : the result is consistent with most observations in supercritical flows. Further the present series of data is in close agreement with shock wave angle at an abrupt channel expansion. The shock wave angle data are best correlated by :

[8] $$\theta = \frac{64.5}{(Fr - 1)^{1.065}}$$ (Data : Present study)

where $\theta$ is in degrees.

## 5. Nappe flow and air entrainment

For one flow rate ($q_w$ = 0.15 $m^2/s$), air concentration distributions were measured in the nappe and downstream of the nappe on the channel centreline and next to the sidewall. Figure 7(a) presents the centreline data while figure 7(b) shows the air concentration profiles 1.7 mm from the sidewall. The un-ventilated air cavity, the impact point and the spray region are indicated. In each figure, dotted lines give the cross-section locations, used as the local zero air content.

The air concentration data highlight the main features of the air-water flow. A large air-cavity is seen beneath the nappe. Nappe subpressure measurement (table 1) indicates that the cavity pressure is nearly atmospheric. The nappe aeration occurs along the sidewall and possibly by free-surface aeration across the upper nappe. The sidewall standing waves and the spray are clearly observed in figure 7(b) and 7(a) respectively. The spray region is characterised by a large amount of flow aeration, with a multitude of water droplets surrounded by air. Downstream of the spray re-attachment, a significant air de-trainment takes place on the centreline. At the end of the invert (i.e. at the downstream overfall), the mean air concentration is still about : $C_{mean}$ = 0.19.

Large amount of entrained are observed near the nappe impact, in the spray region and in the standing waves. Overall the results (fig. 7(a) and 7(b)) highlight the three-dimensional pattern of the air entrainment process.

## 6. Discussion : a prototype experience

A related flow situation was observed at the Gold Creek dam cascade (Chanson and WHITMORE 1996) (fig. 8). The spillway consists of a broad-crest (55-m wide, 61-m long), followed by the remains of the first step (erased in 1975 to enlarge the discharge capacity) and then eleven identical steps (h = 1.5 m, l = 4 m, horizontal steps). On the 2 May 1996 flood waters spilled over the Gold Creek dam spillway following a 200-mm rainfall in twenty-four hours. The first author (Chanson) estimated the discharge as 27 $m^3/s$[1] ($q_w$ = 0.49 $m^2/s$).

The analysis of colour photographs of the operating spillway indicate that (fig. 8):

- the water flows down the chute as a supercritical flow as a succession of free-falling nappes,
- the flow at the first drop is basically two-dimensional and it becomes three-dimensional from the second drop (fig. 8),
- the flow is highly aerated (i.e. 'white waters'),
- free-surface aeration take places downstream of the second drop (fig. 8(a)), and
- at the end of the chute, the distinction between the air-water flow and the spray is impossible and the water surface has a foam appearance (fig. 8(b)).

Further figure 8(b) shows free-surface discontinuities which are characteristic of shock wave intersection next to the step edges. Viewed from downstream (e.g. fig. 8(b)), the free-surface of the upper nappes exhibits a series of lozenges encompassed in between the shock waves. The angle of the shock waves with the flow direction is about 20 to 30 degrees at the downstream end of the spillway. Note that, for such shock wave angles, [8] would predict a flow Froude number of about 3 to 4 (i.e. d ~ 0.12 to 0.14 m).

---

[1]Estimate deduced from photographs taken before, during and after the flood event (in April and May 1996).

CHANSON, H., and TOOMBES, L. (1998). "Supercritical Flow at an Abrupt Drop : Flow Patterns and Aeration." *Can. Jl of Civil Eng.*, Vol. 25, No. 5, Oct., pp. 956-966 (ISSN 0315-1468).

## 7. Conclusions

Supercritical flow at an abrupt drop has been investigated experimentally. The study has highlighted several points :

1- The flow is basically two-dimensional up to the nappe impact and three-dimensional downstream of the nappe impact with formation of shock waves, standing waves and spray.

2- The characteristics of shock waves and standing waves are related to the downstream Froude number Fr and similarity with abrupt expansion supercritical flows is demonstrated.

3- The nappe flow is highly aerated both along the upper and lower free-surfaces.

4- The free-surface aeration of the nappe and the rebounding water tend to affect the shock wave patterns.

5- A prototype cascade overflow exhibited somehow similar features : i.e., substantial free-surface aeration and shock wave development.

The present investigation provides new information on the flow properties of supercritical flows at an abrupt drop. This series of experiments must be extended to predict more accurately the rate of energy dissipation and the complete flow properties of drops and stepped cascades.

## 8. Acknowledgements

The authors acknowledge the assistance of Dr John Macintosh (Water Solutions, Brisbane) and Mr Richard Tumman (Brookfield QLD, Australia). They thank Dr J.S. Montes (University of Tasmania, Australia) for alerting them of the work of late Professor Francisco Javier Dominguez. They acknowledge also the support of the Department of Civil Engineering at the University of Queensland for providing the experimental facility and the financial support of Australian Research Council (Ref. No. A89331591).

## 9. Appendix A - Alternate depths in open channel flow

Considering an open channel flow in a rectangular channel, the continuity and the Bernoulli equations state:

[A1] $q_W = V * d$

[A2] $H - Z_o = d + \frac{V^2}{2 * g}$

where $q_W$ is the discharge per unit width, d is the flow depth, V is the flow velocity, H is the mean total head, $Z_o$ is the bed elevation and g is the gravity constant. The Bernoulli equation (eq. (A2)) is developed assuming a flat horizontal channel, hydrostatic pressure distribution and uniform velocity distribution.

For a given specific energy ($E = H - Z_o$) and flow rate $q_W$, the system of two equations (A1) and (A2) has zero, one or two solutions depending upon the sign of $(H - Z_o - 3/2 * \sqrt[3]{q_W^2/g})$. For a positive term, the two possible solutions correspond to a subcritical flow (i.e. $Fr = q_W/\sqrt{g*d^3} < 1$) and to a supercritical flow.

For a given specific energy and known discharge, the Bernoulli equation is a polynomial equation of degree 3 :

[A3] $\left(\frac{d}{d_c}\right)^3 - \frac{H - Z_o}{d_c} * \left(\frac{d}{d_c}\right)^2 + \frac{1}{2} = 0$

where $d_C = \sqrt[3]{q_W^2/g}$ is the critical flow depth. The three solutions may be expressed in terms of the Froude number :

[A4] $Fr^{(1)} = \left(\frac{H - Z_o}{d_C} * \left(\frac{1}{3} + \frac{2}{3} * \cos\left(\frac{\Gamma}{3}\right)\right)\right)^{-3/2}$ Subcritical flow

[A5] $Fr^{(2)} = \left(\frac{H - Z_o}{d_C} * \left(\frac{1}{3} + \frac{2}{3} * \cos\left(\frac{\Gamma}{3} + \frac{2*\pi}{3}\right)\right)\right)^{-3/2}$ Complex number

[A6] $Fr^{(3)} = \left(\frac{H - Z_o}{d_C} * \left(\frac{1}{3} + \frac{2}{3} * \cos\left(\frac{\Gamma}{3} + \frac{4*\pi}{3}\right)\right)\right)^{-3/2}$ Supercritical flow

where $\cos\Gamma = 1 - \frac{27}{4} * \left(\frac{d_C}{H - Z_o}\right)^3$.

In summary, the downstream ideal flow Froude number in supercritical flow is :

[A5] $Fr = \left(\frac{E_o + h}{d_C} * \left(\frac{1}{3} + \frac{2}{3} * \cos\left(\frac{\Gamma}{3} + \frac{4*\pi}{3}\right)\right)\right)^{-3/2}$ Ideal-fluid flow

where $E_o$ is the upstream specific energy (i.e. $E_o = d_o + 0.5*V_o^2/g$), h is the drop height and $d_C$ is the critical flow depth for a horizontal channel assuming hydrostatic pressure distribution.

## 10. References

Chanson, H. 1995. Air Bubble Entrainment in Free-surface Turbulent Flows. Experimental Investigations. Report CH46/95, Department of Civil Engineering, University of Queensland, Australia, June, 368 pages.

Chanson, H., and Toombes, L. 1997. Flow Aeration at Stepped cascades. Research Report No. CE155, Department of Civil Engineering, University of Queensland, Australia, June, 110 pages.

Chanson, H., and Whitmore, R.L. 1996. Investigation of the Gold Creek Dam Spillway, Australia. Research Report No. CE153, Department of Civil Engineering, University of Queensland, Australia, 60 pages.

Chanson, H., and Whitmore, R.L. (1998). "Gold Creek Dam and its Unusual Waste Waterway (1890-1997) : Design, Operation, Maintenance." *Can. Jl of Civil Eng.*, Vol. 25, No. 4, Aug., pp. 755-768 & Front Cover.

Dominguez, F.J. 1974. Hidraulica. ('Hydraulics.') Editorial Universitataria, Santiago, Chile, 4th edition (in Spanish).

Hager, W.H., and Mazumder, S.K. 1992. Supercritical Flow at Abrupt Expansions. Proceedings of Institution of Civ. Engineers Wat. Marit. & Energy, UK, Vol. 96, Sept., pp. 153-166.

Mazumder, S.K., and Hager, W.H. 1993. Supercritical Expansion Flow in Rouse Modified and Reversed Transitions. Journal of Hydraulic Engineering, ASCE, Vol. 119, No. 2, pp. 201-219.

Schwalt, M., and Hager, W.H. 1993. Supercritical Flow Deflection. Proceedings of 25th IAHR Congress, Tokyo, Japan, Session A, Vol. I, pp. 345-352.

CHANSON, H., and TOOMBES, L. (1998). "Supercritical Flow at an Abrupt Drop : Flow Patterns and Aeration." *Can. Jl of Civil Eng.*, Vol. 25, No. 5, Oct., pp. 956-966 (ISSN 0315-1468).

## 11. List of symbols

| | |
|---|---|
| C | air concentration defined as the volume of air per unit volume of air and water; it is also called void fraction; |
| $C_{mean}$ | mean air concentration defined in term of 90% air content : $C_{mean} = \frac{1}{Y_{90}} * \int_0^{Y_{90}} C * dy$; |
| d | flow depth (m) measured perpendicular to the flow direction; |
| $(d_M)_{int}$ | maximum height (m) at the shock wave intersection on the channel centreline; |
| $(d_M)_{wall}$ | maximum height (m) of the sidewall standing wave; |
| $d_c$ | critical flow depth (m) : $d_c = \sqrt[3]{q_w^2/g}$ in rectangular channel; |
| $d_o$ | flow depth (m) at the channel intake; |
| E | mean specific energy (m); |
| $E_o$ | upstream specific energy (m); |
| Fr | 1- Froude number defined as : $Fr = q_w/\sqrt{g*d^3}$ ;<br>2- downstream Froude number; |
| g | gravity constant : g = 9.80 m/s$^2$ in Brisbane, Australia; |
| H | mean total head (m); |
| h | step height (m); |
| $(L_M)_{wall}$ | distance (m) from the vertical face of the step of the maximum sidewall height; |
| $L_{drop}$ | drop length (m) of the free-falling nappe; |
| $(L_{sw})_{int}$ | distance (m) from the vertical face of the step of the shock wave intersection on the channel centreline; |
| $(L_{sw})_{wall}$ | distance (m) from the vertical face of the step of the sidewall inception at the sidewall; |
| l | step length (m); |
| $q_w$ | water discharge per unit width (m$^2$/s); |
| $t_{wall}$ | thickness (m) of the sidewall standing wave at the maximum height of the standing wave; |
| V | mean velocity (m/s); |
| $V_o$ | mean flow velocity (m/s) at channel intake; |
| W | channel width (m); |
| $W_o$ | inflow channel width (m); |
| x | horizontal distance along the flow direction (m); |
| $Y_{90}$ | characteristic air-water flow depth (m) where C = 0.9; |
| y | vertical distance (m) measured normal to the channel bottom; |
| Z | altitude (m) or vertical elevation positive upwards; |
| $Z_o$ | bed elevation (m); |
| z | distance (m) from the sidewall, measured normal to the sidewall (and to the flow direction); |
| $\Delta P$ | nappe cavity subpressure (Pa); |
| $\Gamma$ | dimensionless parameter; |
| $\theta$ | shock wave angle with the flow direction; |
| $\varnothing$ | diameter (m); |

CHANSON, H., and TOOMBES, L. (1998). "Supercritical Flow at an Abrupt Drop : Flow Patterns and Aeration." *Can. Jl of Civil Eng.*, Vol. 25, No. 5, Oct., pp. 956-966 (ISSN 0315-1468).

*Subscript*

| | |
|---|---|
| int | flow conditions at the shock wave intersection; |
| o | intake flow conditions; |
| wall | flow conditions at the sidewall; |

*Abbreviations*

| | |
|---|---|
| T.H.L | Total Head Line. |

Table 1 - Experimental flow conditions

| Ref. | $q_w$ | $V_o$ | $d_o$ | $\Delta P$ | Comments |
|---|---|---|---|---|---|
| | $m^2/s$ | m/s | m | Pa | |
| (1) | (2) | (3) | (4) | (5) | (6) |
| Present study | | | 0.03 | | W = 0.5 m. h = 0.131 m. Horizontal steps. |
| | 0.038 | 1.27 | | 150 | Supercritical flow u/s and d/s of the drop. |
| | 0.080 | 2.7 | | 138 | Idem. |
| | 0.130 | 4.3 | | 31.3 | Idem. |
| | 0.150 | 5.0 | | 32.8 | Idem. |
| | 0.163 | 5.4 | | -- | Idem. Loud noise generated by air cavity at first drop. |

Notes : $d_o$ : approach flow depth; h : step height; $q_w$ : water discharge per unit width; $\Delta P$ : nappe subpressure.

Table 2 - Analysis and re-analysis of experimental data of shock waves in supercritical flows

| Type of flow | Reference | Flow conditions | Remarks |
|---|---|---|---|
| (1) | (2) | (3) | (4) |
| Abrupt drop | Present study | $Fr_o$ = 2.3 to 10, $d_o$ = 0.03 m, W = 0.5 m | Laboratory experiments in a rectangular channel. |
| Abrupt channel expansion | Hager and Mazumder (1992) | $Fr_o$ = 3.4 to 18.2, $d_o$ = 0.024 to 0.096 m, $W_o$ = 0.25 & 0.5 m, $W/W_o$ = 2, 3 & 5 | Laboratory experiments in a horizontal rectangular channel. |
| Channel expansion | Mazumder and Hager (1993) | Modified Rouse type : $Fr_o$ = 8, $d_o$ = 0.048 m, $W_o$ = 0.5 m, $W/W_o$ = 3, Reverse Rouse type : $Fr_o$ = 4, $d_o$ = 0.096 m, $W_o$ = 0.5 m, $W/W_o$ = 3 | Laboratory experiments in a horizontal rectangular channel. |
| Channel junction | Schwalt and Hager (1993) | $Fr_o$ = 2.5 to 12, $d_o$ = 0.02 to 0.10 m $W_o$ = W = 0.5 m, 30-degree junction (lateral inflow = outflow) | Laboratory experiments in a horizontal rectangular channel. |

Notes : $Fr_o$ : inflow Froude number; $W_o$ : inflow width; W : downstream width.

CHANSON, H., and TOOMBES, L. (1998). "Supercritical Flow at an Abrupt Drop : Flow Patterns and Aeration." *Can. Jl of Civil Eng.*, Vol. 25, No. 5, Oct., pp. 956-966 (ISSN 0315-1468).

Fig. 1 - Sketches of typical flow patterns on the first steps

(a) Flow pattern for $q_W < 0.13$ m$^2$/s ($d_C/h < 0.839$)

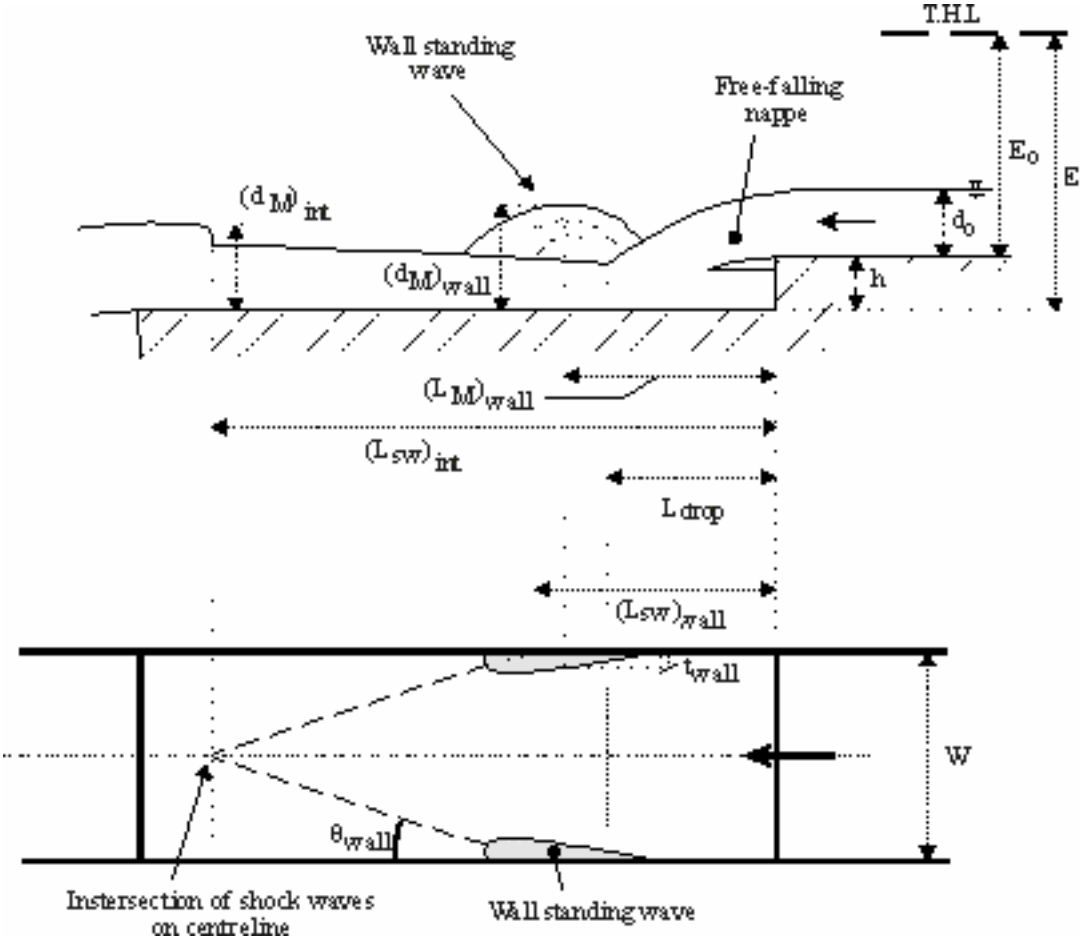


(b) Flow pattern for $q_W = 0.13$ m$^2$/s ($d_C/h = 0.839$)

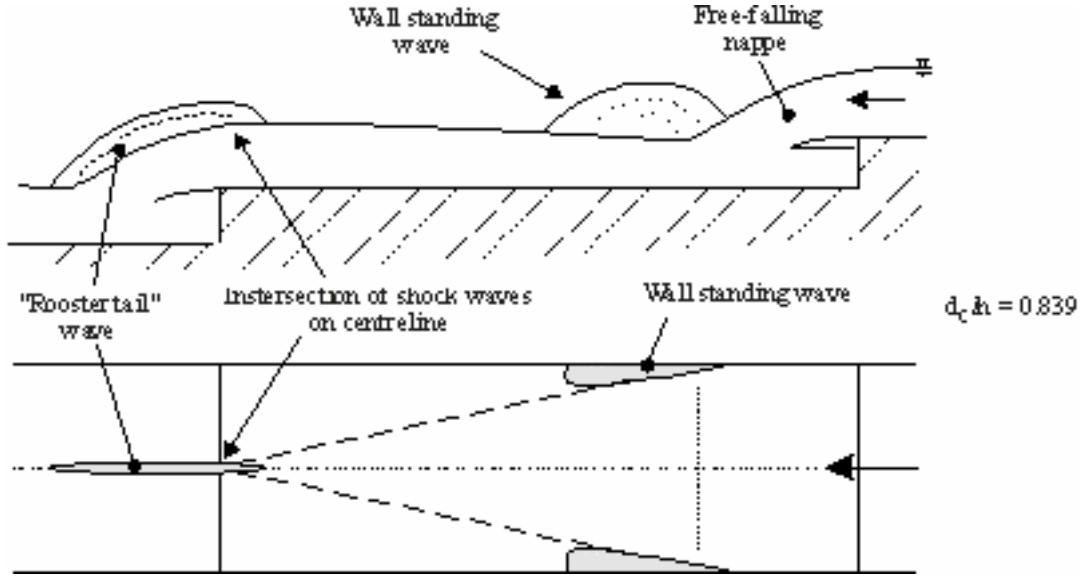

CHANSON, H., and TOOMBES, L. (1998). "Supercritical Flow at an Abrupt Drop : Flow Patterns and Aeration." *Can. Jl of Civil Eng.*, Vol. 25, No. 5, Oct., pp. 956-966 (ISSN 0315-1468).

(c) Flow pattern for $q_W > 0.13$ m$^2$/s ($d_C/h > 0.839$)

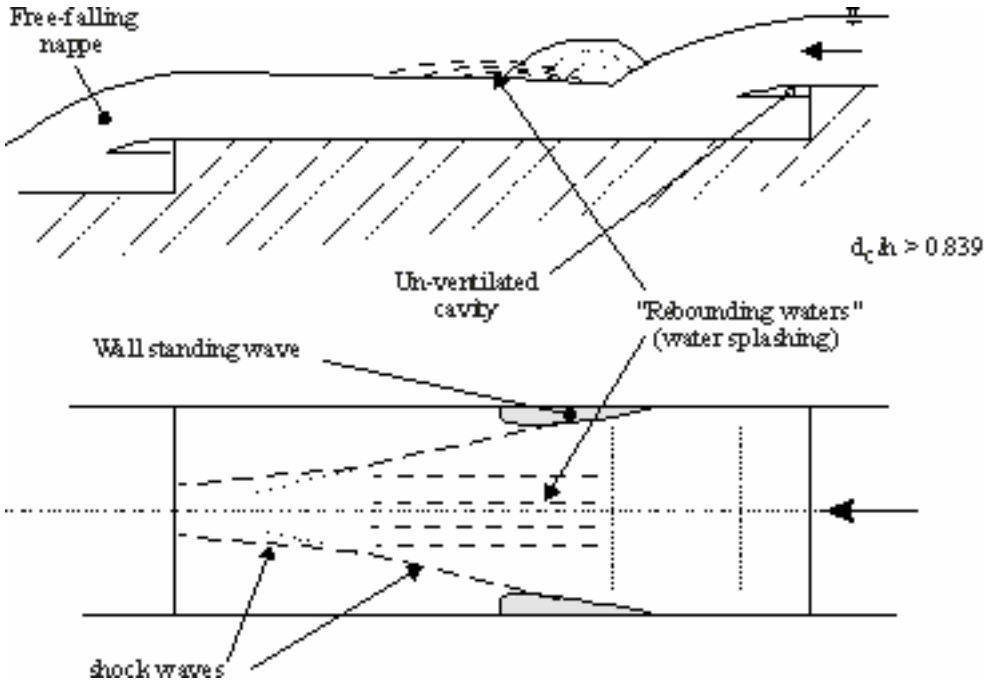

CHANSON, H., and TOOMBES, L. (1998). "Supercritical Flow at an Abrupt Drop : Flow Patterns and Aeration." *Can. Jl of Civil Eng.*, Vol. 25, No. 5, Oct., pp. 956-966 (ISSN 0315-1468).

Fig. 2 - Photographs of oblique shock waves and sidewall standing waves

(a) Oblique shock waves downstream of the drop ($d_C/h = 0.87$) - Flow from bottom to top - High-speed photographs taken at night (67 μs flash speed) (b) Sidewall standing waves downstream of the drop ($d_C/h = 0.77$) - Flow from left to right (c) Oblique shock waves downstream of the drop with rooster tail wave developing downstream of the shock wave intersection and onto the second overfall ($d_C/h = 0.91$) - Flow from bottom to top (d) Oblique shock waves with a broken line shape near the downstream overfall ($d_C/h = 0.92$) - Flow from bottom to top - High-speed photographs taken at night (67 μs flash speed)

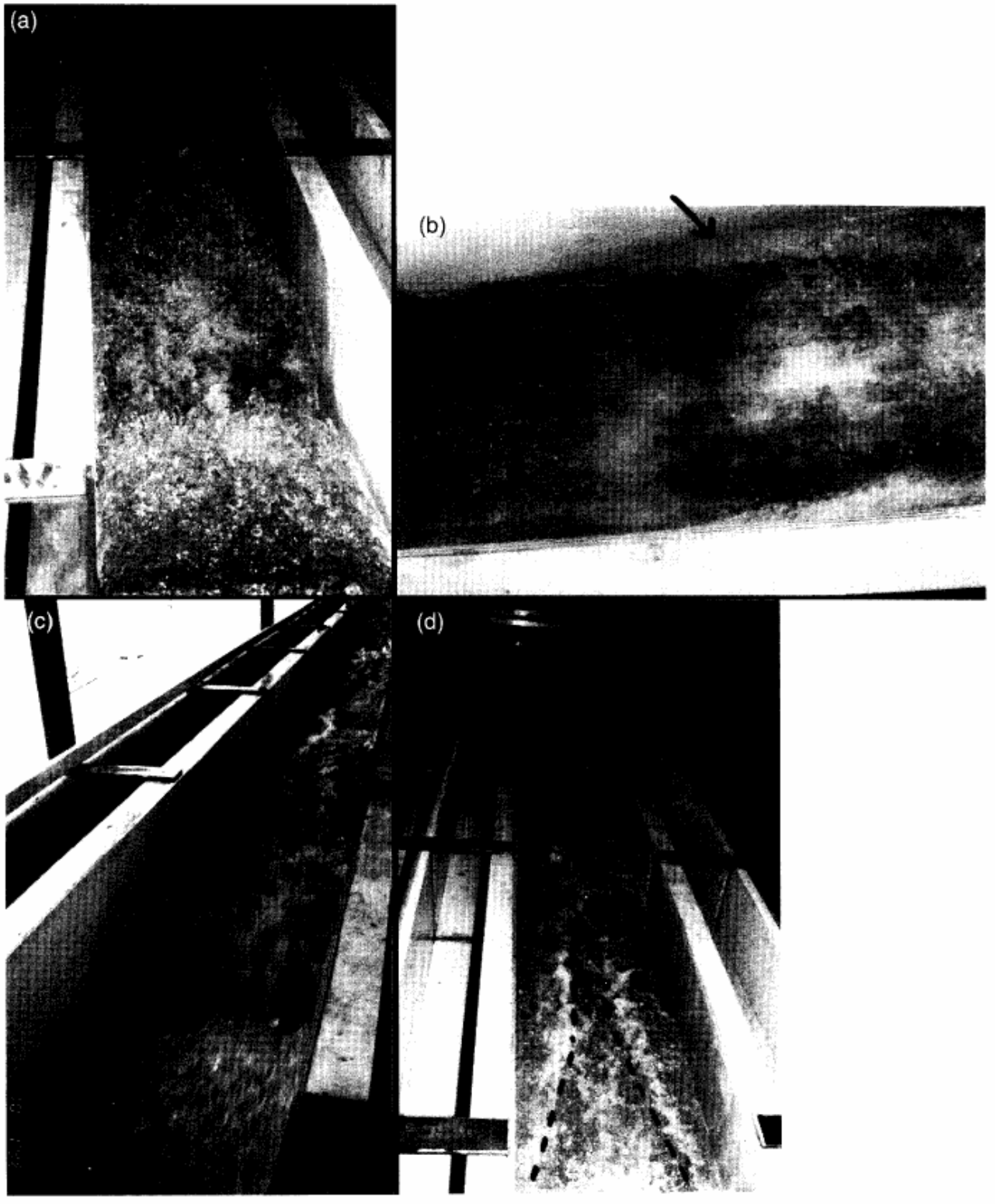

CHANSON, H., and TOOMBES, L. (1998). "Supercritical Flow at an Abrupt Drop : Flow Patterns and Aeration." *Can. Jl of Civil Eng.*, Vol. 25, No. 5, Oct., pp. 956-966 (ISSN 0315-1468).

Fig. 3 - Dimensionless lengths at the first drop as functions of the downstream Froude number (ideal flow) : drop length $L_{drop}/W$, position of the maximum standing wave height $(L_M)_{wall}/W$, position of the start of shock waves at wall $(L_{sw})_{wall}/W$, position of intersection of shock waves $(L_{sw})_{int}/W$

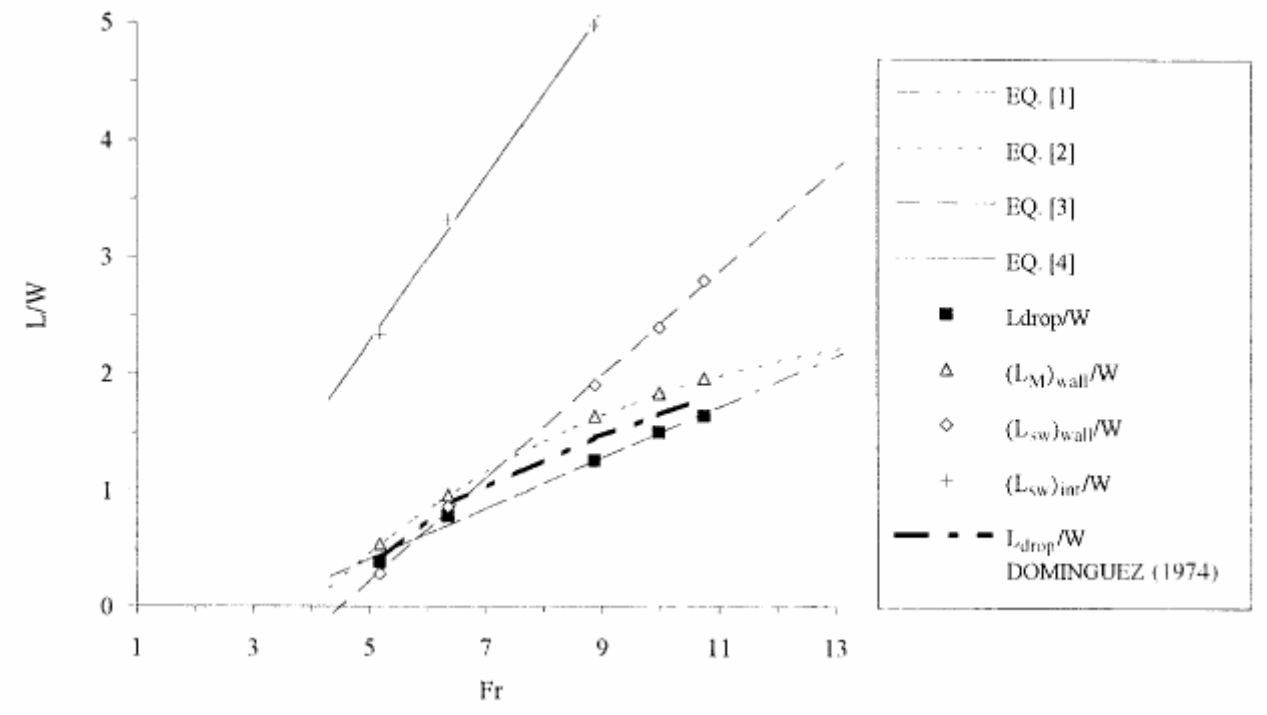


Fig. 4 - Dimensionless maximum free-surface heights at the wall $(d_M)_{wall}/E$ and at the intersection of shock waves on the channel centreline $(d_M)_{int}/E$ as functions of the downstream Froude number (ideal flow) (table 3)

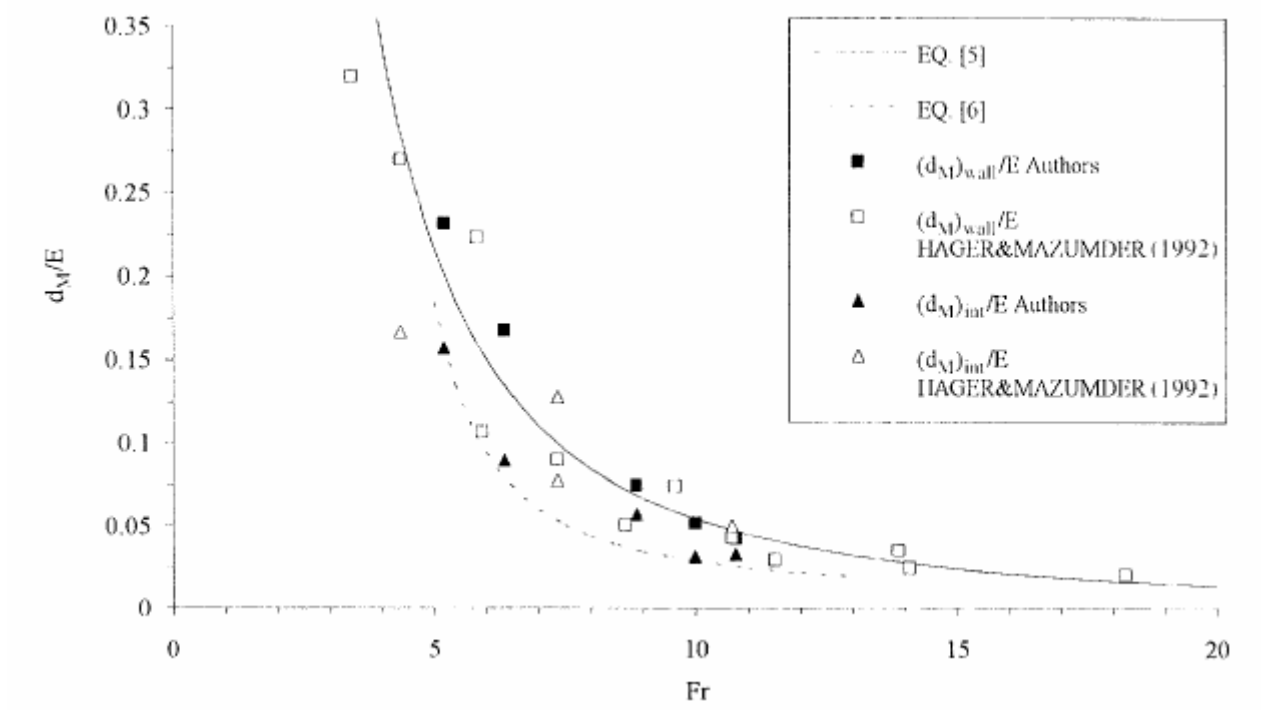

CHANSON, H., and TOOMBES, L. (1998). "Supercritical Flow at an Abrupt Drop : Flow Patterns and Aeration." *Can. Jl of Civil Eng.*, Vol. 25, No. 5, Oct., pp. 956-966 (ISSN 0315-1468).

Fig. 5 - Dimensionless thickness of the sidewall standing wave at the maximum free-surface height at wall $t_{wall}/E$ as a function of the downstream Froude number (ideal flow) (table 3)

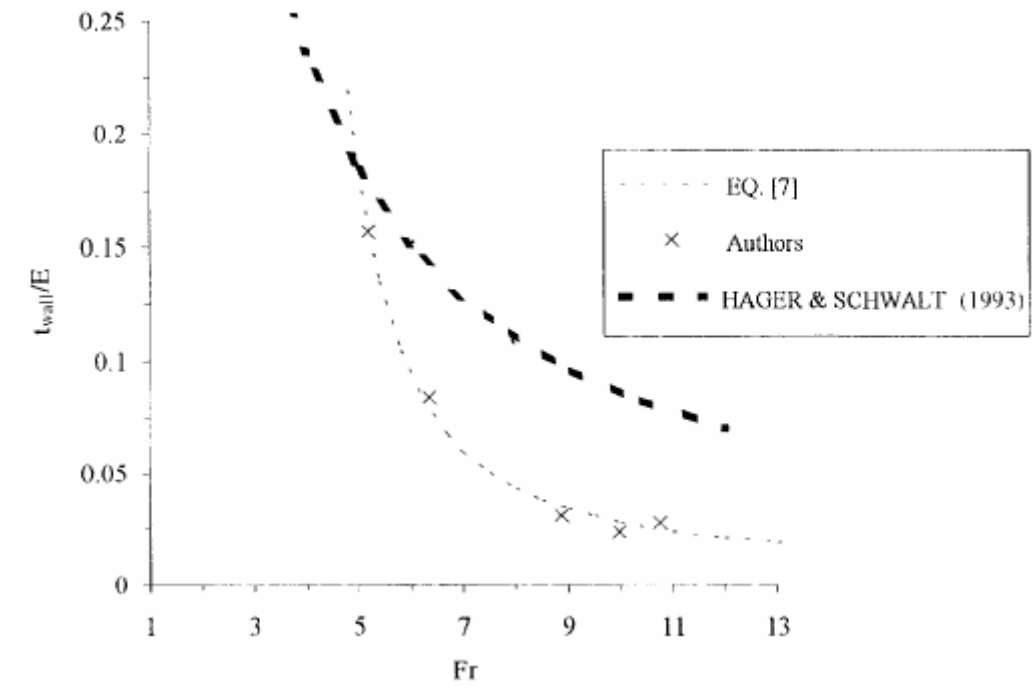


Fig. 6 - Shock wave angle with sidewall $\theta_{wall}$ a function of the downstream Froude number (ideal flow) (table 3)

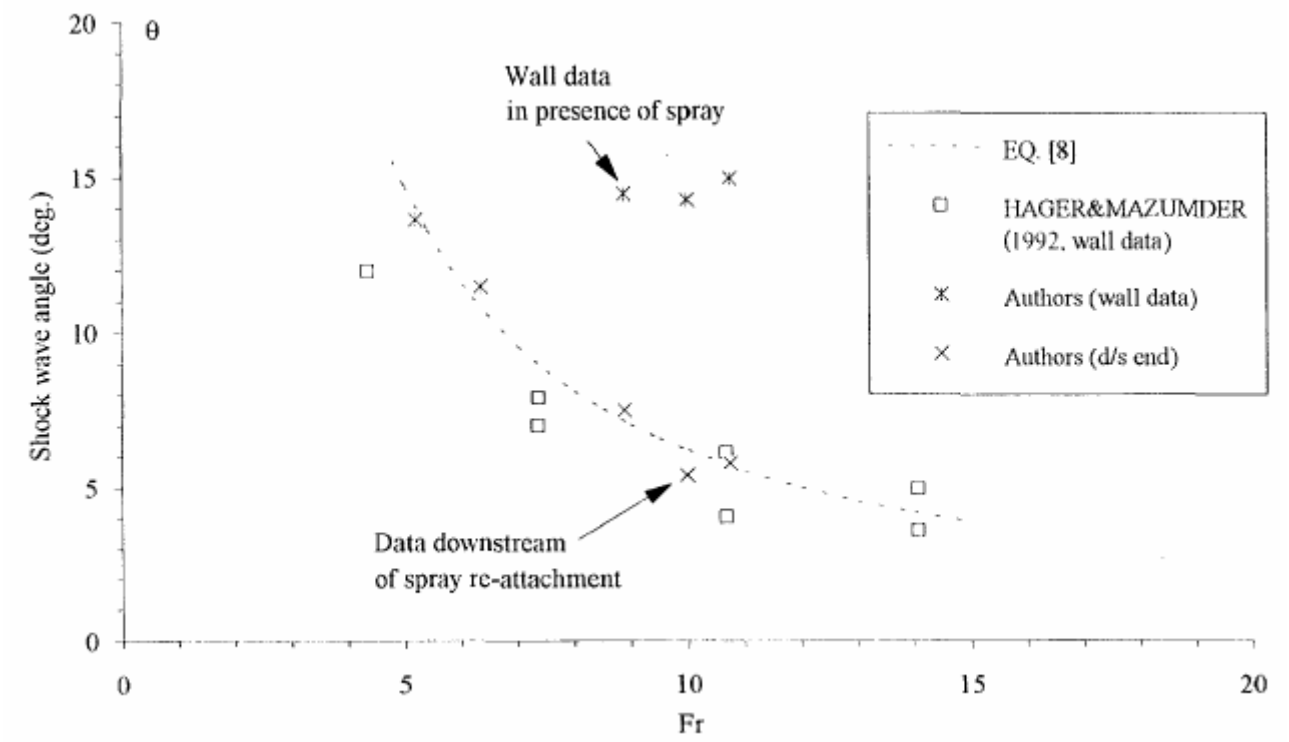

CHANSON, H., and TOOMBES, L. (1998). "Supercritical Flow at an Abrupt Drop : Flow Patterns and Aeration." *Can. Jl of Civil Eng.*, Vol. 25, No. 5, Oct., pp. 956-966 (ISSN 0315-1468).

Fig. 7 - Air concentration measurement in supercritical flow at an abrupt drop

(a) $q_W$ = 0.15 $m^2$/s, centreline data

(b) $q_W$ = 0.15 $m^2$/s, measurements at 1.7 mm from the sidewall

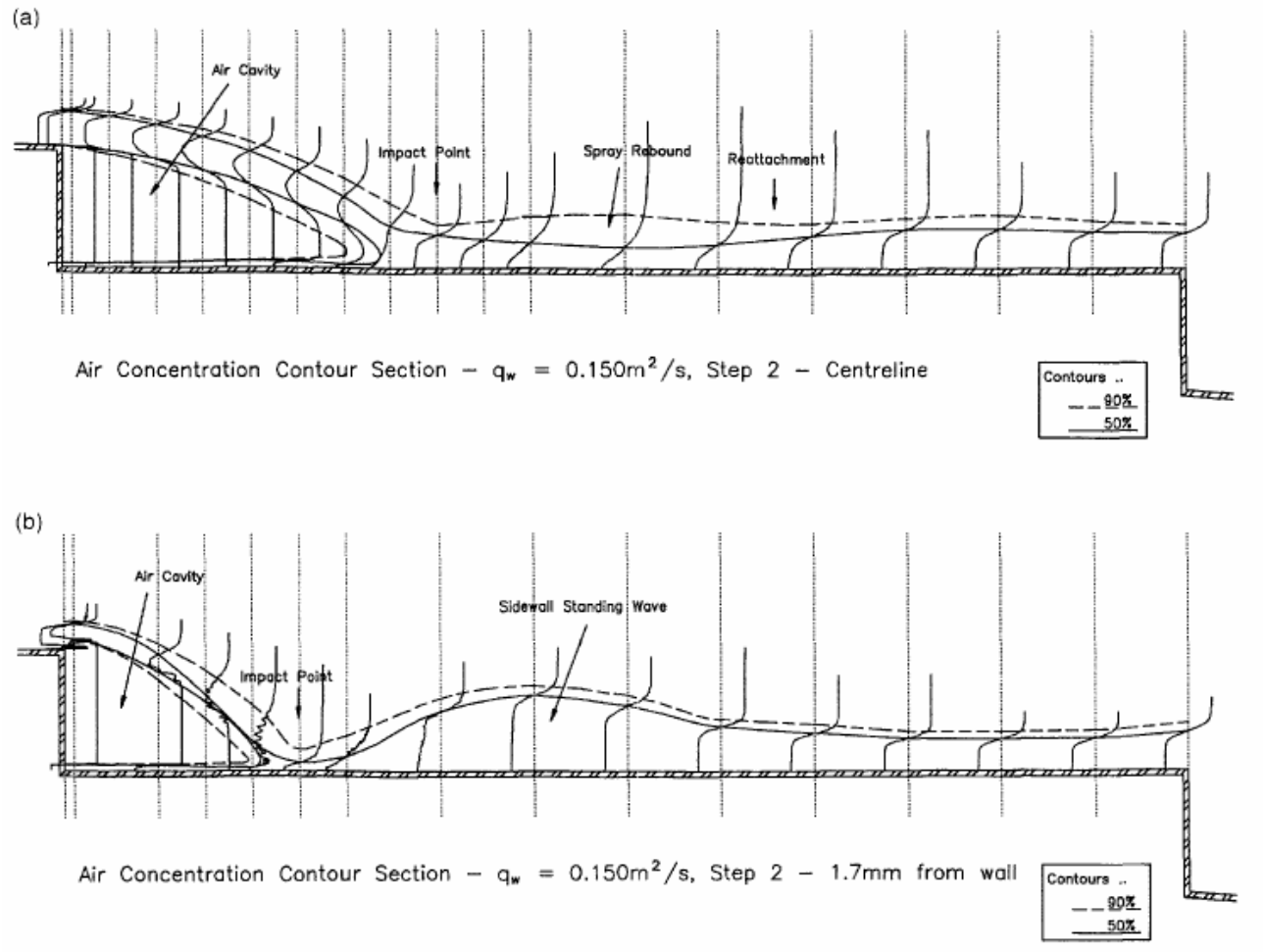

CHANSON, H., and TOOMBES, L. (1998). "Supercritical Flow at an Abrupt Drop : Flow Patterns and Aeration." *Can. Jl of Civil Eng.*, Vol. 25, No. 5, Oct., pp. 956-966 (ISSN 0315-1468).

Fig. 8 - Nappe flow above the Gold Creek dam spillway, on 2 May 1996 (discharge : 27 $m^3/s$)

Spillway characteristics : h = 1.5 m, 20.6 degree slope, W = 55 m, maximum discharge capacity : 280 $m^3/s$, built in 1890 (un-reinforced concrete steps)

(a) View from the right bank, near the crest. Flow from the left bottom corner to the top right corner. Note the flow past the first small drop (remains of first step) which is not aerated.

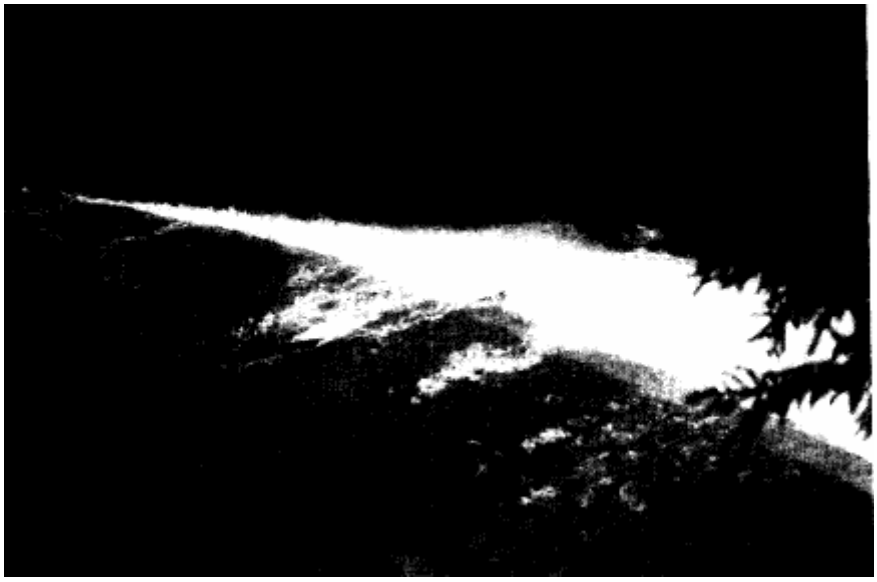

CHANSON, H., and TOOMBES, L. (1998). "Supercritical Flow at an Abrupt Drop : Flow Patterns and Aeration." *Can. Jl of Civil Eng.*, Vol. 25, No. 5, Oct., pp. 956-966 (ISSN 0315-1468).

Fig. 8 - Nappe flow above the Gold Creek dam spillway, on 2 May 1996 (discharge : 27 $m^3/s$)

Spillway characteristics : h = 1.5 m, 20.6 degree slope, W = 55 m, maximum discharge capacity : 280 $m^3/s$, built in 1890 (un-reinforced concrete steps)

(b) View from downstream. At the end of the chute the flow turns to the right (i.e. left of the photograph) and there is no dissipation structure. Note cross-waves intersecting at the step edges and on the free-falling nappes and the resulting lozenge flow pattern.